ORIGINAL RESEARCH

Mitogen-Activated Protein Kinase–Activated Protein Kinase 2 Mediates Apoptosis during Lung Vascular Permeability by Regulating Movement of Cleaved Caspase 3

Mahendra Damarla[1], Ahmad R. Parniani[2], Laura Johnston[1], Hasina Maredia[3], Leonid Serebreni[1], Omar Hamdan[1], Venkataramana K. Sidhaye[1], Larissa A. Shimoda[1], Allen C. Myers[1], Michael T. Crow[1], Eric P. Schmidt[4], Carolyn E. Machamer[5], Matthias Gaestel[6], Madhavi J. Rane[2], Todd M. Kolb[1], Bo S. Kim[1], Rachel L. Damico[1], and Paul M. Hassoun[1]

[1]Department of Medicine, Johns Hopkins University School of Medicine, Baltimore, Maryland; [2]University of Louisville, School of Medicine, Louisville, Kentucky; [3]Brown University, Providence, Rhode Island; [4]Department of Medicine, University of Colorado School of Medicine, Aurora, Colorado; [5]Department of Cell Biology, Johns Hopkins University School of Medicine, Baltimore, Maryland; and [6]Department of Biochemistry, Medical School of Hannover, Hannover, Germany

Abstract

Apoptosis is a key pathologic feature in acute lung injury. Animal studies have demonstrated that pathways regulating apoptosis are necessary in the development of acute lung injury, and that activation of p38 mitogen-activated protein kinase (MAPK) is linked to the initiation of the apoptotic cascade. In this study, we assessed the role of the MAPK-activated protein kinase (MK) 2, one of p38 MAPK's immediate downstream effectors, in the development of apoptosis in an animal model of LPS-induced pulmonary vascular permeability. Our results indicate that wild-type (WT) mice exposed to LPS demonstrate increased apoptosis, as evidenced by cleavage of caspase 3 and poly (ADP-ribose) polymerase 1 and increased deoxynucleotidyl transferase–mediated dUDP nick-end labeling staining, which is accompanied by increases in markers of vascular permeability. In contrast, $MK2^{-/-}$ mice are protected from pulmonary vascular permeability and apoptosis in response to LPS. Although there was no difference in activation of caspase 3 in $MK2^{-/-}$ compared with WT mice, interestingly, cleaved caspase 3 translocated to the nucleus in WT mice while it remained in the cytosol of $MK2^{-/-}$ mice in response to LPS. In separate experiments, LPS-induced apoptosis in human lung microvascular endothelial cells was also associated with nuclear translocation of cleaved caspase 3 and apoptosis, which were both prevented by MK2 silencing. In conclusion, our data suggest that MK2 plays a critical role in the development of apoptosis and pulmonary vascular permeability, and its effects on apoptosis are in part related to its ability to regulate nuclear translocation of cleaved caspase 3.

Keywords: apoptosis; lung injury; caspase 3; nuclear translocation; kinases

Acute lung injury (ALI) is a devastating illness, with an annual incidence of 200,000 and a mortality rate upwards of 40% (1). Most commonly seen in the setting of sepsis (2, 3), ALI is a complex syndrome marked by increased vascular permeability causing tissue edema and profound hypoxia (4) as a result of interstitial inflammation and disruption of the endothelial vascular barrier (5, 6). There are no directed therapies for ALI, and treatment remains largely supportive (5).

Recent studies investigating the pathogenesis of ALI have demonstrated that apoptosis is a major feature of lung injury (6–12). Apoptosis is a highly regulated process where proapoptotic signals cleave and activate caspases, which act to both amplify death stimuli via initiator caspases and ultimately dismantle the cell via the effector caspases (13). Inhibiting apoptosis, via inhibiting caspase activity, prevents lung injury, suggesting a necessary role for caspase activation in the development of apoptosis-induced lung injury (7, 14, 15).

Several recent publications have implicated p38 mitogen-activated protein kinase (MAPK) in the pathogenesis of ALI (7, 12, 16, 17). Furthermore, activation of p38 MAPK has been linked to the initiation of proapoptotic cascades, leading to cell death (12, 18, 19). Our laboratory has recently shown that p38 MAPK is both upstream and necessary for activation of the executioner caspases 3 and 7 and

(Received in original form August 15, 2013; accepted in final form November 16, 2013)

Correspondence and requests for reprints should be addressed to Mahendra Damarla, M.D., Department of Medicine, Division of Pulmonary and Critical Care Medicine, 5501 Hopkins Bayview Circle, Baltimore, MD. E-mail: mdamarl1@jhmi.edu

This article has an online supplement, which is accessible from this issue's table of contents at www.atsjournals.org

Am J Respir Cell Mol Biol Vol 50, Iss 5, pp 932–941, May 2014

Originally Published in Press as DOI: 10.1165/rcmb.2013-0361OC on December 4, 2013
Internet address: www.atsjournals.org

eventual apoptosis. Moreover, inhibiting p38 MAPK abrogates caspase 3/7 activity and prevents apoptosis *in vivo* (7). The MAPK-activated protein kinase (MK) 2, a well described substrate of p38, is phosphorylated and activated by p38 MAPK in response to cellular stress (20). Recently, Shiroto and colleagues (21) demonstrated that $MK2^{-/-}$ mice exhibit decreased numbers of cardiomyocytes undergoing apoptosis in response to myocardial ischemia–reperfusion injury. The mechanism(s) by which MK2 deficiency is protective against apoptosis is not known. Furthermore, the ability of MK2 to interact with the molecular machinery of apoptosis (i.e., caspase activation) has not been evaluated. As such, we tested the hypothesis that MK2 is necessary for activation of the apoptotic cascade (i.e., caspase 3 cleavage) and resultant apoptosis during endotoxemia-induced pulmonary vascular permeability.

Materials and Methods

The Johns Hopkins University Institutional Animal Care and Use Committee approved all animal protocols. Detailed methods are in the online supplement.

Male C57BL/6J (wild-type [WT]) mice, aged 10–12 weeks (Jackson Laboratory, Bar Harbor, ME) and $MK2^{-/-}$ mice, C57BL/6J background (20), were exposed to intravenous PBS or LPS (0127:B8, product no. L3129; Sigma, St. Louis, MO) via retro-orbital injection (22) for up to 24 hours.

Histology

Lung tissue sections were incubated with antibodies against cleaved caspase 3 (Cell Signaling, Cambridge, MA). Negative antibody controls revealed no staining. Nuclear staining was achieved with 4′,6-diamidino-2-phenylindole or To-Pro1. Confocal images were pseudocolored. Quantification of colocalization of cleaved caspase 3 and nuclear staining was performed using ImageJ (Bethesda, MD).

Markers of Apoptosis

Apoptosis was measured by terminal deoxynucleotidyl transferase–mediated dUDP nick-end labeling (TUNEL) staining, DeadEnd Colorimetric TUNEL System (Promega, Madison, WI), and the presence of DNA laddering using Apoptotic DNA Ladder Detection Kit II (Promokine, Heidelberg, Germany).

Caspase 3/7 activity was measured using Caspase-Glo 3/7 Assay (Promega).

Immunoblot Analysis

Phospho-specific and anti–total antibodies directed at p38, MK2, heat shock protein (HSP)27 (Cell Signaling, Boston, MA), and HSP25 (Abcam, Cambridge, MA), as well as antibodies directed against cleaved caspase 3, total caspase 3, poly (ADP-ribose) polymerase 1 (PARP1; Cell Signaling) and Rho-associated, coiled-coil containing protein kinase 1 (ROCK1; Abcam) were used. Manufacturer-generated positive controls are denoted as positive, unless otherwise indicated.

Nuclear and cytosolic fractionation. Lungs were flushed free of blood, harvested, and then mashed through a 70-μm nylon cell strainer (BD Falcon, Franklin Lakes, NJ). Nuclear and cytosolic fractions of the resulting cell suspensions were generated using NE-PER Nuclear and Cytoplasmic Extraction Reagents (Thermo Fisher Scientific, Rockford, IL).

Reagents and Tissues

Human lung microvascular endothelial cells. Human lung microvascular endothelial cells (HMVECs) derived from individual donors (Lonza, Walkersville, MD) were maintained in complete media with 10% FBS and analyzed between passages 7 and 9. HMVECs were placed in basal media, 1% FBS supplementation, overnight and LPS (25 ng/ml) was added for up to 16 hours. Control cells had PBS added.

Short interfering RNA. Duplex RNAs encoding nontargeting short interfering RNA (siRNA) (On-Target Plus; denoted siRNA-Scrambled) and siRNA directed against human MK2 were used for RNA interference (Dharmacon, Inc., Lafayette, CO). Four duplex siRNAs targeting MK2 were screened. siRNA number J-003516-13 (sequence, GGCAUCAACGGCAAAGUUU) had the most effect in MK2 suppression (data not shown), and was used for knockdown studies.

Human tissues. Deidentified lung samples with diffuse alveolar damage were obtained from the Department of Pathology archives of the University of Colorado, as previously described (23). Control lung tissues were collected from deidentified organ donors procured by the International Institute for the Advancement of Medicine (Exton, PA), or the National Disease Research Institute (Philadelphia, PA).

Statistical Analysis

Data are shown as means (± SEM). Comparison between two groups was performed using *t* tests. We performed multiple comparisons by ANOVA with Tukey's *post hoc* testing. For comparisons between groups, two-way ANOVA was performed to detect differential effects of LPS with *post hoc t* testing. A P value of less than 0.05 was considered significant. Data were analyzed using GraphPad Prism 4 (La Jolla, CA).

Results

Intravenous LPS Induces Pulmonary Vascular Permeability

Because sepsis is one of the most common precipitating causes of ALI (2, 3), we created a murine model of endotoxemia-induced pulmonary vascular permeability to recapitulate the early signaling events in sepsis-induced ALI. Adult male WT mice were subjected to intravenous PBS or LPS at increasing doses for 6 hours. This time point was chosen on the basis of prior published work (24). As shown in Figures 1A and 1B, there is a dose-dependent increase in the amount of Evans blue dye (EBD) extravasation and wet-to-dry lung weight ratios. There was no statistical difference in the amount of capillary leakage in mice exposed to 7.5 mg/kg of LPS compared with 10 mg/kg of LPS.

Intravenous LPS Induces Apoptosis within the Lung

As shown in Figure 1C, there is marked cleavage (i.e., activation) of caspase 3 in total lung homogenates after 6 hours of exposure to intravenous LPS as compared with PBS. The antibody against total caspase 3 recognizes both the total, pro–caspase 3 (∼ 34 kD), as well as cleaved caspase 3, which is comprised of the approximately 17-kD fragment and the large fragment that is still associated with the prodomain (∼ 19 kD) (25). To determine if the activation of the apoptotic cascade (i.e., cleavage of caspase 3) in fact culminated in apoptosis, TUNEL staining was performed. There was a marked increase in the amount of TUNEL-positive cells in lung tissue sections of mice exposed to intravenous LPS as compared with

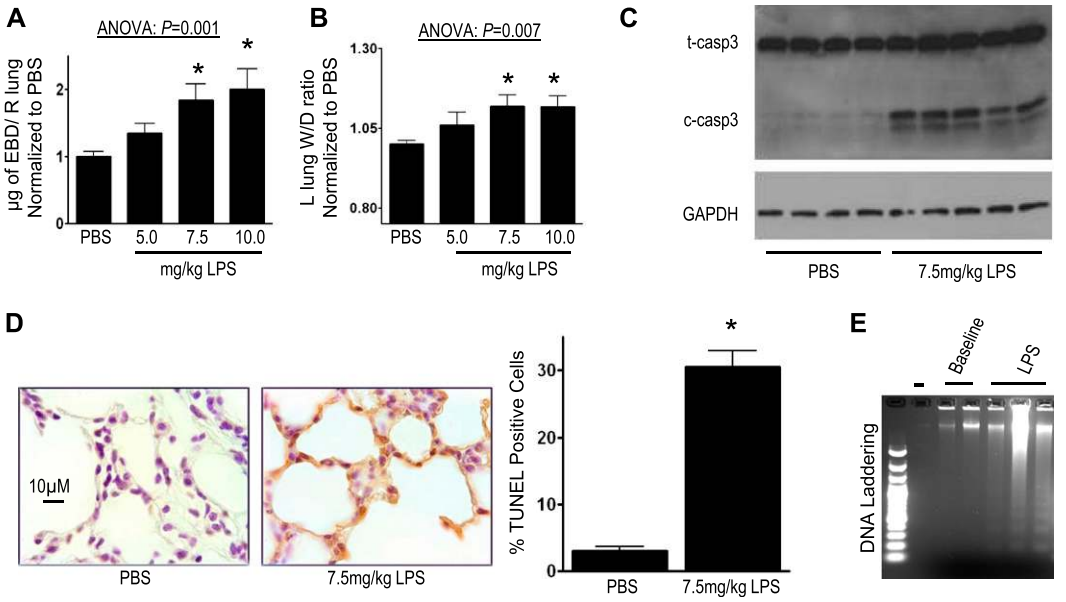

Figure 1. Intravenous exposure to LPS induces lung injury and apoptosis in mice. C57BL/6J mice were exposed to intravenous LPS or PBS for 6 hours and lung tissue was harvested for evidence of lung injury and apoptosis. (*A*) Mice exposed to varying concentrations of intravenous LPS demonstrate a dose-dependent increase in Evans blue dye (EBD) extravasation, with no significant increase above 7.5 mg/kg of LPS. (*B*) The wet-to-dry (W/D) lung weight ratios were also increased in a dose-dependent manner with no significant increase above 7.5 mg/kg of LPS. (*C*) Lung tissue homogenates from mice exposed to PBS or LPS were immunoblotted with antibodies recognizing total caspase 3. As shown, there is a significant cleavage of caspase 3, as evidenced by increase in the two lower bands, which are comprised of the large fragment, roughly 17 kD, and the large fragment that is still associated with the prodomain, roughly 19 kD. (*D*) Deoxynucleotidyl transferase–mediated dUDP nick-end labeling (TUNEL) staining of lung tissue sections from mice exposed to PBS or LPS for 6 hours (*left panels*). Quantification of TUNEL staining reveals a significant increase in TUNEL-positive staining in mice exposed to LPS compared with PBS. More than 1,500 events were counted from random images of four or five mice per group. (*E*) Gel electrophoretic analysis of DNA isolated from lungs of mice treated with LPS demonstrates a ladder pattern compared with lungs at baseline. *$P < 0.05$ versus PBS. −, water alone (negative control); c-, cleaved; GAPDH, glyceraldehyde 3-phosphate dehydrogenase; R, right; t-, total.

PBS (Figure 1D). As TUNEL-positive staining can also result from other forms of cell death (i.e., necrosis), we assessed for DNA laddering from the DNA isolated from lungs of mice exposed to LPS to confirm that the positive TUNEL staining resulted from apoptosis. As shown in Figure 1E, there is significant DNA laddering, signifying internucleosomal degradation of DNA characteristic of apoptosis, in lungs of mice exposed to LPS. Finally, to demonstrate that caspase-dependent apoptosis is a pathogenic factor in this model of LPS-induced pulmonary vascular permeability, we inhibited apoptosis with the broad-spectrum caspase inhibitor, z-ASP. As shown in Figure E1A in the online supplement, the LPS-induced increase in EBD extravasation is completely abrogated with z-ASP pretreatment.

MK2 Is Necessary for LPS-Induced Pulmonary Vascular Permeability and Apoptosis

Immunoblot analyses demonstrated that intravenous LPS induces phosphorylation of HSP25, the phosphorylation target of MK2, whereas $MK2^{-/-}$ mice are unable to phosphorylate HSP25 (Figure 2A). As shown in Figures 2B and 2C, $MK2^{-/-}$ mice exposed to intravenous LPS are almost completely protected from pulmonary vascular permeability, as evidenced by the lack of EBD lung extravasation and changes in lung wet-to-dry weight ratios. Having demonstrated that $MK2^{-/-}$ mice are protected from pulmonary vascular permeability in response to intravenous LPS, we then investigated the role of MK2 on LPS-induced apoptosis. As shown in Figure 2D, there is no increase in TUNEL-positive staining in response to intravenous LPS in $MK2^{-/-}$ mice as compared with their WT counterparts, demonstrating a protection from intravenous LPS-induced apoptosis. Next, we sought to confirm the role of MK2 in activation of the apoptotic cascade. Surprisingly, $MK2^{-/-}$ mice were still able to activate caspase 3 in response to intravenous LPS (Figure 2E), despite the absence of increased apoptosis (Figure 2D), suggesting a dissociation between activation of the apoptotic cascade and the execution of apoptosis in these mice.

MK2 Is Necessary for Nuclear Translocation of Cleaved Caspase 3

As nuclear translocalization of active caspase 3 has been reported to be necessary for the execution of apoptosis, and defective nuclear translocalization of cleaved caspase 3 is a potential mechanism of apoptosis resistance (26–30), we investigated the role of MK2 in nuclear translocalization of cleaved caspase 3. There was diffuse cellular staining of total caspase 3 in lung sections of WT mice under PBS conditions, which did not change with LPS exposure (Figure E2A). There was minimal lung immunohistochemical staining for the cleaved specific isoform of caspase 3 in WT mice after exposure to PBS (data not shown), consistent with the immunoblot analysis of Figure 1C. Interestingly, after intravenous LPS exposure in WT mice, staining for cleaved caspase 3 directly overlies the nucleus, whereas in $MK2^{-/-}$ mice it remained essentially within the

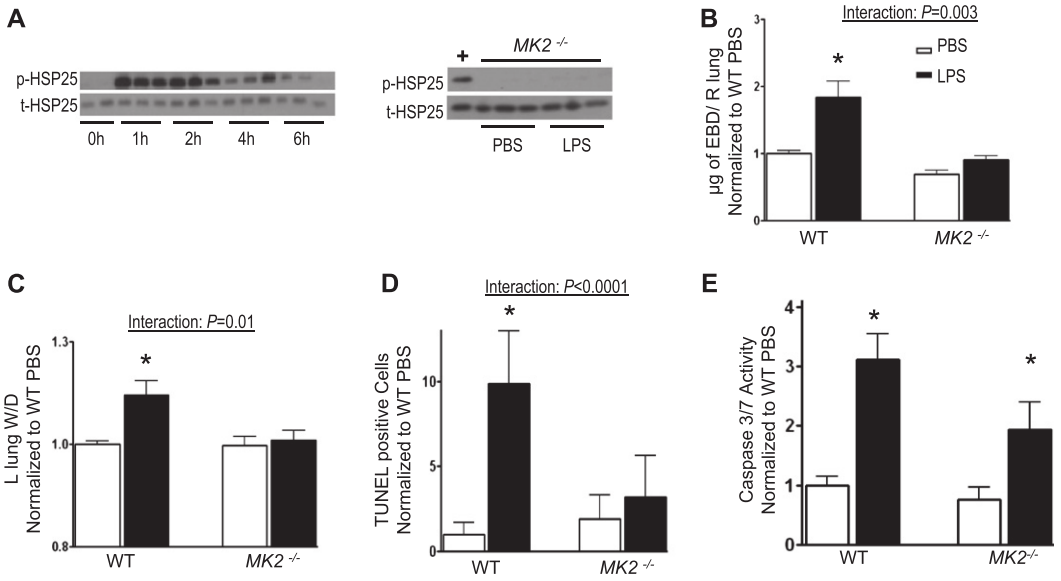

Figure 2. Mitogen-activated protein kinase (MAPK)-activated protein kinase (MK) 2 is necessary for lung injury and apoptosis in response to LPS. Wild-type (WT) or *MK2*$^{-/-}$ mice were exposed to 7.5 mg/kg intravenous LPS or PBS for up to 6 hours and lung tissue was harvested for markers of lung injury and evidence of apoptosis. (*A*) WT mice were exposed to LPS for up to 6 hours, after which lungs were harvested for protein analysis. Representative immunoblots of three mice per time point. *Left panel*: Heat shock protein (HSP)25 is phosphorylated in response to LPS, with a peak phosphorylation at 1–2 hours. *Right panel*: *MK2*$^{-/-}$ mice fail to phosphorylate HSP25 after exposure to LPS. +, lung homogenate from WT mice after 2 hours of LPS exposure. (*B* and *C*) *MK2*$^{-/-}$ mice do not exhibit increase in lung injury in response to intravenous LPS compared with WT mice: EBD extravasation (*B*), lung wet-to-dry weight ratios (*C*). (*D*) TUNEL staining of lung tissue sections from WT and *MK2*$^{-/-}$ mice exposed to PBS or LPS for 6 hours demonstrates a significant increase in WT mice in response to LPS, but there is no increase in TUNEL staining in *MK2*$^{-/-}$ mice. More than 3,000 events were counted from random images of four or five mice per group. (*E*) There is no differential caspase 3/7 activation in response to LPS in WT and *MK2*$^{-/-}$ mice (two-way ANOVA, interaction $P > 0.05$). Caspase 3/7 activity is increased similarly in WT and *MK2*$^{-/-}$ mice after 6 hours of LPS exposure. n = 4–8 mice per group; *$P < 0.05$ versus PBS.

cytosol after intravenous LPS exposure, Figure 3A. To quantitatively assess any difference in nuclear localization of cleaved caspase 3 in WT and *MK2*$^{-/-}$ mice after LPS exposure, confocal laser immunofluorescent microscopy was used. As shown in Figure 3B, there was nearly a 30-fold difference in the number of colocalized pixels of cleaved caspase 3 and nuclear staining in WT and *MK2*$^{-/-}$ mice, suggesting a critical defect in nuclear localization of cleaved caspase 3 in *MK2*$^{-/-}$ mice. We further explored this phenomenon using immunoblotting techniques.

As we are interested in early signaling events leading to increased apoptosis and vascular permeability, and were intrigued by the effect of MK2 on caspase 3 activation, we initially performed a time course of PARP1 cleavage. As shown in Figure E2B, there was a significant increase in cleaved PARP1 after 2 hours of LPS exposure. We chose this time point for further analyses. Nuclear and cytosolic fractionations of lung tissue obtained after 2 hours of intravenous LPS exposure, a time of significant cleavage of lung PARP1, demonstrated clear evidence of cytosolic as well as nuclear cleaved caspase 3 in WT mice (Figure 3C). The large fragment that is still associated with the prodomain (~ 19-kD fragment) is the one that preferentially localized to the nuclear fraction, suggesting that translocalization of cleaved caspase 3 is an active and selective process, and not merely occurring by passive diffusion. Interestingly, both the roughly 19-kD and roughly 17-kD fragments of cleaved caspase 3 in *MK2*$^{-/-}$ mice remained in the cytosolic fraction (Figure 3C), consistent with the imaging findings. Immunoblot analysis of the nuclear fractions over a time course demonstrated minimal cleaved caspase 3 in the nucleus at baseline, with further accumulation over time (Figure E2C), suggesting progression of translocalization of cleaved caspase 3 in WT mice, in response to intravenous LPS.

To further confirm differential localization of cleaved caspase 3 between WT and *MK2*$^{-/-}$ mice in response to LPS, we assessed for functional activity of caspase 3 within cytosolic and nuclear compartments. There was a substantial increase in cleavage of ROCK1, a cytosolic substrate of caspase 3, in both WT and *MK2*$^{-/-}$ mice in response to LPS, demonstrating that there is functional active/cleaved caspase 3 in the cytosolic compartment (Figure 4A and Figure E2E) and in accordance with the imaging data showing cleaved caspase 3 within the cytosolic compartment in both WT and *MK2*$^{-/-}$ mice (Figure 3). Interestingly, there is a differential response to LPS based on genotype—WT versus *MK2*$^{-/-}$—in the cleavage of ROCK1 (Figure 4A, two-way ANOVA, $P = 0.001$), suggesting increased cleavage of ROCK1 (i.e., increased cytoplasmic activity of caspase 3) in *MK2*$^{-/-}$ mice as compared with WT mice. We then determined whether the nuclear substrate of caspase 3, PARP1, was affected. WT mice demonstrated a significant increase in cleavage of PARP1 in response to LPS, suggesting caspase 3 translocation to the nucleus. In contrast, although there was evidence of baseline cleaved PARP1 (with PBS exposure) in *MK2*$^{-/-}$ mice (further suggesting disassociation of "molecular

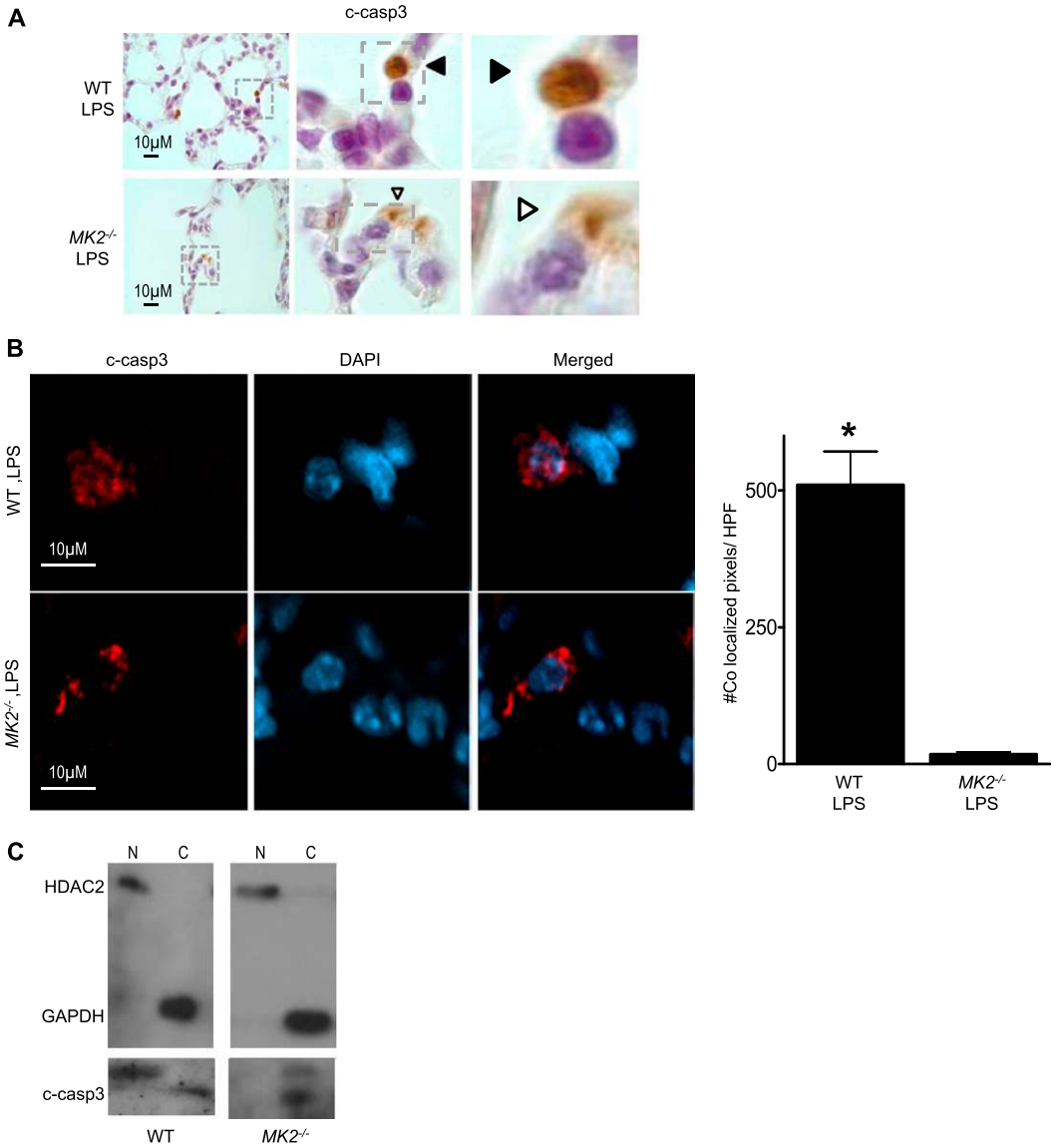

Figure 3. MK2 is necessary for nuclear translocation of cleaved caspase 3 in response to LPS. (*A*) After exposure to LPS for 6 hours, staining for cleaved specific caspase 3 in WT mice (*black arrowheads*) reveals concentrated staining overlying the nucleus. In *MK2*$^{-/-}$ mice, staining is diffuse and primarily excluding the nucleus (*white arrowheads*). *Dashed insets* are optically zoomed. (*B*) Confocal laser microscopy demonstrates that cleaved specific caspase 3 (*red staining*) in WT mice in response to LPS is intranuclear (*blue staining*) as well as cytosolic. In *MK2*$^{-/-}$ mice, cleaved caspase 3 is primarily cytosolic. Quantification of colocalization of cleaved caspase 3 and nuclear staining demonstrates a nearly roughly 30-fold increase in WT mice compared with *MK2*$^{-/-}$ mice. More than 250 images were analyzed. Representative images taken at 40× magnification and optically zoomed. *$P < 0.05$. (*C*) Nuclear and cytosolic fractions from lung tissue of WT mice exposed to LPS for 2 hours reveals that the roughly 19-kD fragment of cleaved caspase 3 is within the nuclear fraction, whereas the roughly 17-kD fragment remains within the cytosolic fraction. In *MK2*$^{-/-}$ mice exposed to 2 hours of LPS, both the roughly 19-kD and the roughly 17-kD fragments of cleaved caspase 3 are within the cytosolic fraction. Purity of nuclear and cytosolic fractions was assessed by exclusion of GAPDH and HDAC2 immunoblotting, respectively. Representative immunoblot of three mice per condition. C, cytosolic; HPF, high power field; N, nuclear.

activation" of the apoptotic cascade and apoptosis), this was not increased in response to intravenous LPS (Figure 4B and Figure E2F). Collectively, these data show nuclear localization of cleaved caspase 3 over time in response to LPS in WT mice, but not in *MK2*$^{-/-}$ mice (Figure 3), consistent with the imaging data.

To confirm that MK2 deficiency did not merely delay nuclear translocalization of cleaved caspase 3, we extended our studies from early time points of 2 and 6 hours to also include 24 hours. We measured the activity of caspase 3 within nuclear fractions after 24 hours of intravenous LPS exposure. As shown in Figure 4C, the total lung lysates from WT and *MK2*$^{-/-}$ mice show a similar increase in caspase 3/7 activity in response to intravenous LPS. However, in sharp contrast, nuclear caspase 3/7 activity from the WT mice was significantly increased (close to fourfold) in response to LPS, whereas there was no change in *MK2*$^{-/-}$ mice (Figure 4C, two-way ANOVA,

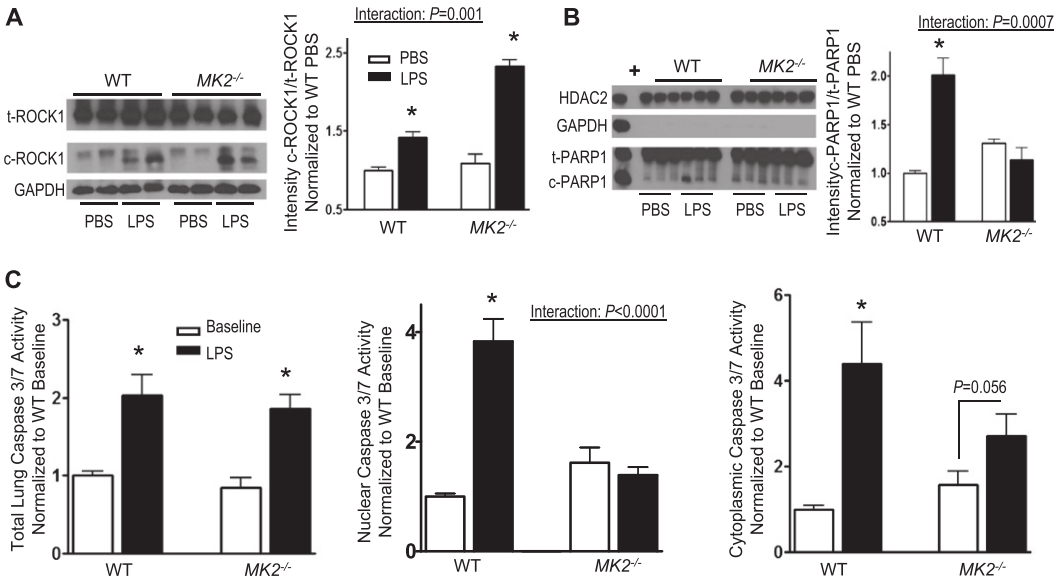

Figure 4. MK2 is necessary for caspase 3 activity within the nucleus in response to LPS. (*A*) *Left panel*: representative immunoblot of lung tissue homogenates of mice exposed to LPS for 6 hours indicates an increase in cleavage of Rho-associated, coiled-coil containing protein kinase 1 (ROCK1) in both WT and $MK2^{-/-}$ mice in response to LPS. Densitometric analysis confirms a differential response to LPS based on genotype in the cleavage of ROCK1 (two-way ANOVA, $P = 0.001$), indicating increased cleavage of ROCK1 in $MK2^{-/-}$ mice as compared with WT mice (*right panel*); $n = 3$ mice per condition. (*B*) *Left panel*: representative immunoblot of nuclear and cytosolic fractions from lung tissue of mice exposed to PBS or LPS for 2 hours indicates an increase in cleavage of poly (ADP-ribose) polymerase 1 (PARP1) in WT in response to LPS, but not $MK2^{-/-}$ mice, confirmed by densitometric analysis (*right panel*). Purity of nuclear and cytosolic fractions was assessed by exclusion of GAPDH and HDAC2 immunoblotting, respectively. C, cytosolic; N, nuclear; $n = 3$ mice per condition. (*C*) After exposure to 10 mg/kg of LPS for 24 hours, lungs were harvested and nuclear and cytosolic fractions were separated. *Left panel*: total lung lysates from WT and $MK2^{-/-}$ mice after 24 hours of LPS exposure demonstrate a similar increase in caspase 3/7 activity. *Middle panel*: the nuclear fractions of lung tissue from these same mice demonstrate that WT mice show a significant increase in nuclear caspase 3/7 activity. There is no increase in nuclear caspase 3/7 activity in $MK2^{-/-}$ in response to LPS. *Right panel*: the cytosolic fractions from these mice demonstrate no differential effect of LPS based on genotype, and that there is a significant increase in caspase 3/7 in WT, whereas the increase in caspase 3/7 activity in $MK2^{-/-}$ mice reaches borderline statistical significance. $n = 5$–6 mice per condition. $^*P < 0.05$ versus PBS/baseline.

interaction $P < 0.0001$), further suggesting that MK2 plays a pivotal role in nuclear translocation of cleaved caspase 3. In the cytosolic fractions, there was not a differential effect of LPS on the increase in caspase 3/7 activity based on genotype (two-way ANOVA, interaction $P > 0.05$). There was a significant increase in caspase 3/7 activity in WT, whereas the increase was borderline significant in $MK2^{-/-}$ mice ($P = 0.056$). Despite that borderline increase in cytosolic caspase 3/7 activity in $MK2^{-/-}$ mice in response to LPS when measured using activity assays, the *in situ* functional cytosolic caspase 3 activity was significantly higher in $MK2^{-/-}$ than WT mice (Figure 4A).

Role of MK2 in Apoptosis in Human Tissues

To test the interspecies relevance of our results, we sought to replicate these findings in human tissues. As our experiments thus far have been performed in whole mouse lungs, the relevant cellular compartment is unclear. We hypothesized that, because our animal preparation mostly models pulmonary vascular permeability, endothelial cells, due to their position, are likely prime targets of intravenous LPS and resulting apoptosis, as previously demonstrated. Despite showing significant increases in pulmonary vascular permeability (lung wet-to-dry weight, EBD extravasation, Figure 1) in response to intravenous LPS, we were unable to demonstrate other classic features of ALI, such as disruption of the epithelial barrier leading to alveolitis (i.e., change in bronchoalveolar lavage fluid protein concentration [Figure E1B] in our model, similar to other reports [31]), suggesting increased interstitial edema, and implicating a critical role for endothelial cells in our model. To that end, we investigated the role of MK2 in activation of the apoptotic cascade as well as the execution of apoptosis in HMVECs. Using incremental doses of LPS, we determined that 25 ng/ml consistently induced apoptosis (data not shown) in HMVECs, as evidenced by nuclear morphological analysis with Hoechst dye 33,342 (Invitrogen, Carlsbad, CA) staining, as previously described (32). We next investigated the activation of the p38 MAPK–MK2–HSP27 signaling cascade in HMVECs in response to LPS. As shown in Figure 5A, p38 MAPK, MK2, and HSP27 (the human homolog of mouse HSP25) have a similar pattern of phosphorylation, demonstrating activation of this pathway in these cells in response to LPS. Caspase 3 is cleaved as early as 1 hour after LPS exposure, with peak cleavage occurring at between 2 and 4 hours, Figure 5B. We subsequently obtained nuclear and cytosolic fractions of HMVECs exposed to LPS to determine whether cleaved caspase 3 translocated to the nucleus. As shown in Figure 5C, there was nuclear localization of cleaved caspase 3 and an increase in PARP1 cleavage after LPS exposure, similar to the murine samples (Figures 3 and 4).

To test the role of MK2 in this *in vitro* model, we exposed cells to LPS and, using

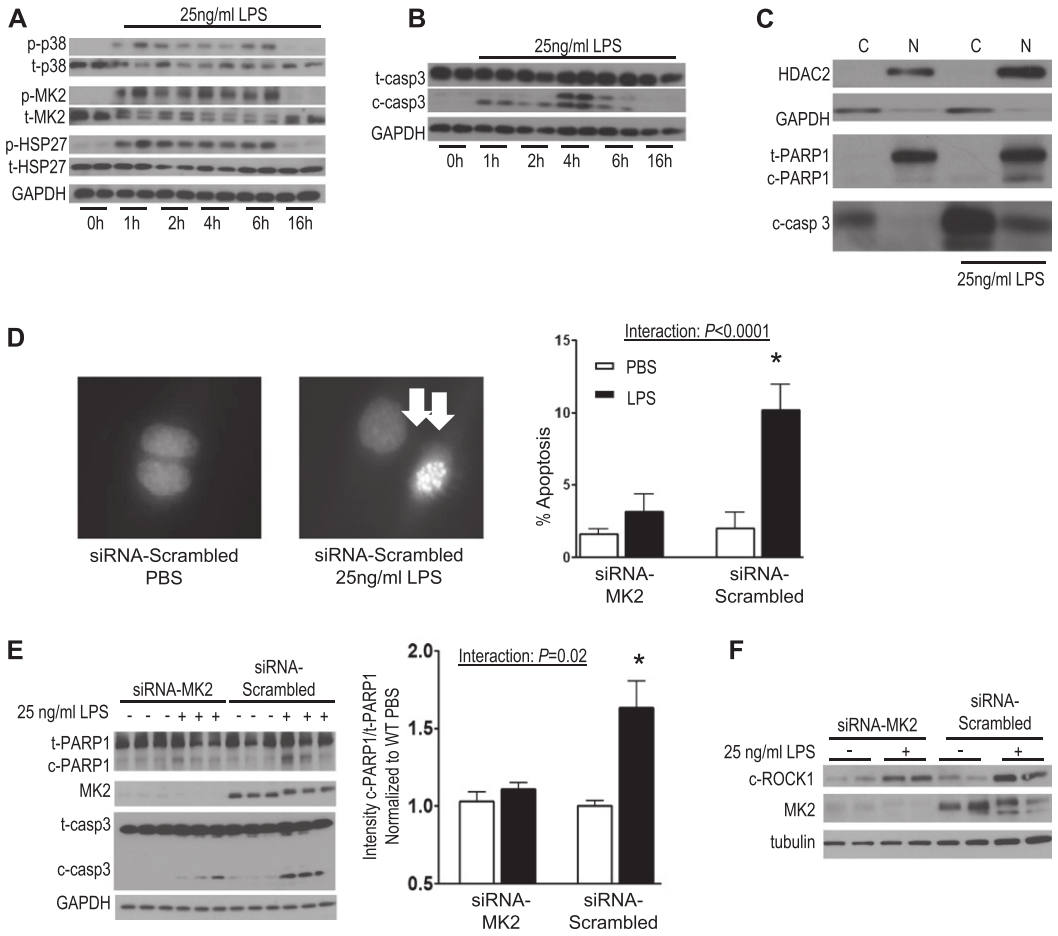

Figure 5. MK2 is necessary for nuclear translocation of cleaved caspase 3 and apoptosis in human microvascular endothelial cells (HMVECs) in response to LPS. HMVECs were exposed to 25 ng/ml of LPS or vehicle for up to 16 hours, after which cells were harvested for various analyses. (*A*) p38 MAPK, MK2, and HSP27 are phosphorylated in response to LPS, with an initial phosphorylation at 1 hour and a return to the unphosphorylated state by 16 hours. The doublet seen in the t-MK2 row (only when there is p-MK2) represents both the phosphorylated and unphosphorylated states of MK2. Representative immunoblots of three separate experiments. (*B*) There is a significant cleavage of caspase 3 in response to LPS. (*C*) Nuclear and cytosolic fractions of HMVECs exposed to LPS for 3 hours (approximate time of peak cleavage of caspase 3) reveals increased cleavage of PARP1 and the roughly 19-kD fragment of cleaved caspase 3 within the nuclear fraction. Representative immunoblot of three separate experiments. (*D*) HMVECs were exposed to short interfering RNA (siRNA)-scrambled and siRNA-MK2 before LPS exposure and nuclei were stained with Hoechst dye. *Left panels*: fluorescent microscopy reveals apoptotic morphologic changes (i.e., nuclear condensation and fragmentation, *white arrow*). Quantification of apoptotic cell death demonstrates that cells treated with siRNA-MK2 do not show an increase in apoptosis with LPS exposure for 13 hours. Representative of two separate experiments with over 1,300 cells counted per group. (*E*) HMVECs were treated with siRNA targeting MK2 or a nontargeting siRNA (siRNA-Scrambled), and 72 hours later were exposed to LPS for 4 hours. *Left panel*: there is increased cleaved PARP1 with LPS exposure in cells treated with siRNA-Scrambled, but not with siRNA-MK2, even while there is increased cleaved caspase 3. *Right panel*: densitometric analysis confirms increase in cleaved PARP1. (*F*) Cleavage of ROCK1 is increased in response to LPS in cells treated with both siRNA-MK2 and siRNA-Scrambled. *$P < 0.05$ versus PBS. Representative of three separate experiments. p-, phosphorylated.

fluorescent microscopy, assessed for apoptosis by nuclear morphology (Figure 5D). There was increased apoptosis in LPS-exposed cells treated with scrambled siRNA, which was prevented by MK2 suppression using siRNA (Figure 5D).

Next, we investigated the role of MK2 in nuclear translocation of cleaved caspase 3 during apoptosis in HMVECs. As shown in Figure 5E, substantial knockdown of MK2 protein expression with siRNA targeted against MK2 is achieved compared with scrambled siRNA. Furthermore, during WT conditions (siRNA scrambled), there was increased cleaved PARP1 with LPS exposure as compared with PBS exposure. Similar to the *in vivo* findings, there was no increase in cleaved PARP1 with LPS exposure with MK2 knockdown, despite an increase in caspase 3 cleavage (Figure 5E). Although there was slightly less cleavage of caspase 3 with MK2 knockdown, there was still a significant increase in the cleavage of ROCK1 (Figure 5F), a cytosolic substrate of caspase 3, with no increase in the cleavage of the nuclear substrate of caspase 3, PARP1 (Figure 5E), in response to LPS exposure, which is consistent with the *in vivo* findings (Figures 3 and 4).

Little is known about cellular localization of cleaved caspase 3 in humans, in particular under diseased conditions.

Accordingly, we performed immunohistochemical staining of lung tissue sections from patients who died with asthma (non-ALI control), traumatic brain injuries (nonpulmonary disease control), and from patients with diffuse alveolar damage (pathologic hallmark of acute respiratory distress syndrome [ARDS]). There was no appreciable staining for cleaved caspase 3 in lung tissue from control conditions (Figure E3B). However, lung tissue biopsy specimens from patients with ARDS demonstrated clear positive staining for the cleaved specific isoform of caspase 3, which overlies the nucleus in numerous cells (Figure 6A). Using confocal immunofluorescent microscopy, we confirmed that cleaved caspase 3 staining is localized within the nucleus and perinuclear areas (Figure 6B), suggesting nuclear localization of cleaved caspase 3 in human patients with ARDS.

Discussion

This study demonstrates that LPS leads to apoptosis and pulmonary vascular permeability in an *in vivo* murine model of sepsis. LPS exposure activates the p38–MK2–HSP25/27 signaling pathway, as well as the apoptotic cascade. On activation of the apoptotic cascade, cleaved caspase 3 translocates to the nucleus in the execution of apoptosis. MK2 deficiency does not prevent activation of the apoptotic cascade (i.e., there is no attenuation in activity of caspase 3). Rather, MK2 deficiency results in retention within the cytosol of cleaved caspase 3 (the active form), thus preventing its nuclear translocation in response to LPS. Importantly, these data suggest that nuclear translocation of caspase 3, via MK2-dependent mechanisms, is a necessary step for the execution of LPS-induced apoptosis and resultant vascular permeability. Finally, we provide evidence that, in human patients with ARDS, a condition in which apoptosis is a key pathogenic factor (33, 34), cleaved caspase 3 localizes within the nucleus.

It was surprising that MK2 knockdown or deficiency did not protect against activation of the apoptotic cascade. Our group and others have previously shown that p38 MAPK activates the apoptotic cascade (7, 12, 18, 19, 35). Of the four identified isoforms of p38, p38α has been shown to be proapoptotic (36). Specifically, p38 MAPK has been shown to activate the mitochondrial pathway leading to caspase 3 activation (19, 37). HSP27 is protective against apoptosis in response to numerous stimuli *in vitro* and *in vivo* (38–41). HSP27 interacts with the mitochondrial pathway of apoptosis to alter activation of caspase 3 (42–44). Previous work would suggest that MK2, an immediate downstream substrate of p38 MAPK and the immediate upstream kinase known to phosphorylate HSP27, should affect apoptosis by altering caspase 3 activation. We focused our studies on the intersection of MK2 with the apoptotic cascade on caspase 3, as the initiator caspases from both intrinsic and extrinsic pathways culminate in activation of caspase 3. Our data clearly show that with MK2 deficiency, caspase 3 is activated, although there is no increased apoptosis in response to LPS, implicating a protective mechanism downstream of caspase 3 activation (i.e., prevention of nuclear translocation of cleaved caspase 3).

Another rather surprising finding was the cleavage of PARP1 at baseline conditions with MK2 deficiency or knockdown. However, there was no significant increase in cleaved PARP1 relative to total PARP1 under MK2-deficient conditions at baseline, which was corroborated by lack of increased baseline apoptosis (Figures 2D and 5D). These data suggest homeostatic maintenance of PARP1. PARP1 is traditionally thought of as a marker for apoptosis (45–47). In that context, it is noteworthy that PARP1 is a DNA repair enzyme (45, 46, 48), which, when cleaved, becomes unable to participate in the repair of DNA nicks. Thus, if there were minimal DNA damage, as one would expect under baseline conditions, the balance between cleaved and total PARP1 may represent a newly achieved homeostasis specifically attributed to MK2 loss.

Nuclear localization of caspase 3 is thought to occur via passive diffusion, as caspase 3 lacks a typical nuclear localization sequence. Recent studies, however, suggest that nuclear translocation of caspase 3 is in fact an active process in apoptosis (27–29). Furthermore, nuclear translocation of caspase 3 seems to be necessary for the execution of apoptosis (26–30). Kamada

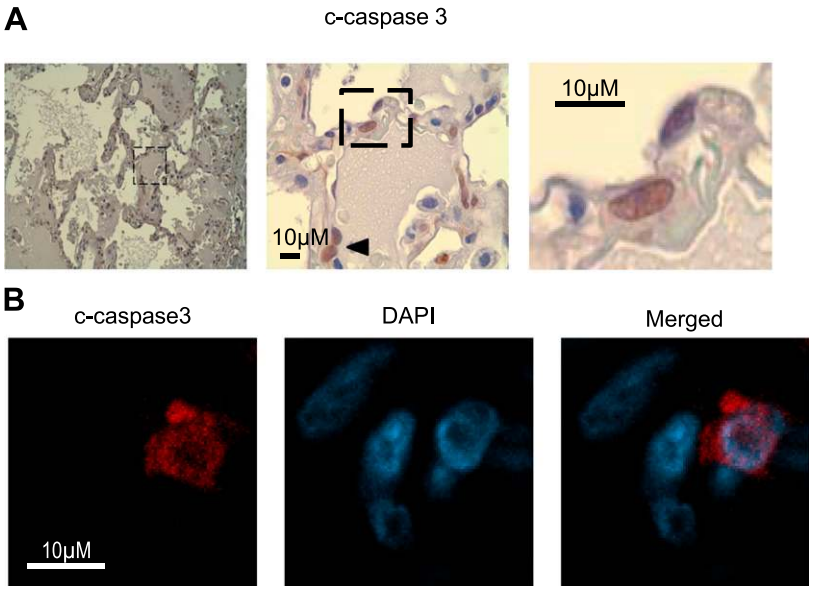

Figure 6. Nuclear localization of cleaved caspase 3 in human patients with diffuse alveolar damage (DAD). Lung biopsy specimens from patients with clinical diagnoses of acute lung injury (ALI) and a pathological DAD were stained for cleaved caspase 3. (*A*) A 48-year-old male with history of bone marrow transplant and lung biopsy specimen consistent with DAD. Immunohistochemical staining for cleaved specific caspase 3 reveals numerous cells staining positively with staining overlying the nucleus (*black arrowhead*). *Dashed inset* has been optically zoomed. (*B*) A 57-year-old male with history of heart transplant with *Escherichia coli* sepsis and lung biopsy specimen consistent with DAD. Confocal laser microscopy confirms cleaved specific caspase 3 is intranuclear as well as cytosolic (*red staining*). Nuclei stained with 4′,6-diamidino-2-phenylindole (DAPI; *blue staining*). Representative images taken at 40× magnification and optically zoomed. Representative of seven different patients.

and colleagues (28) demonstrated that a mutated caspase 3 that is unable to be activated does not translocate to the nucleus on stimulation with anti-fas treatment, implicating proteolytic activation as a necessary step for nuclear translocation. Although activation of caspase 3 is necessary for nuclear translocation, the necessity of cleaved caspase 3's functional activity for nuclear translocation is less certain (28, 30). Despite increased interest in the mechanisms of nuclear translocation of caspase 3, the molecular machinery necessary for this process has not been elucidated. Kamada and colleagues have suggested that A-kinase–anchoring protein 95 (AKAP-95) may act as a molecular chaperone for transporting cleaved caspase 3 to the nucleus; however, no direct evidence that knockdown of AKAP-95 prevented the nuclear translocation of cleaved caspase 3 was presented, and knockdown of AKAP-95 was not consistently cytoprotective (27). Our results clearly show that caspase 3 is activated, translocates to the nucleus, and cleaves its substrates in the apoptotic response in WT conditions in response to LPS. Under MK2-deficient conditions, with the use of $MK2^{-/-}$ mice *in vivo* and siRNA against MK2 *in vitro*, caspase 3 is activated; however, its translocation to the nucleus is inhibited, although it retains its ability to cleave substrates within the cytosolic compartment, suggesting that the cellular localization of caspase 3 is independent of its catalytic activity. Furthermore, apoptosis and lung injury are prevented in MK2-deficient conditions. The mechanism(s) by which MK2 deficiency prevents nuclear translocation of cleaved caspase 3 is/are unclear. We speculate that HSP25/27 may play a critical role, as it is known to bind to the prodomain of caspase 3, and has been shown to translocate to the nucleus in monocytes undergoing spontaneous apoptosis (49). Another potential mechanism of MK2 regulating nuclear translocalization of cleaved caspase 3 is via post-translational modification (i.e., phosphorylation) of caspase 3. As shown in Figure E2D, within the nuclear compartment in WT mice, caspase 3 appears as a triplet with a slightly lower molecular weight compared with the total/unprocessed pro–caspase 3 within the cytosol; these findings are absent in $MK2^{-/-}$ mice. These data suggest that caspase 3 is a potential substrate of MK2 and, once modified (i.e., phosphorylated), undergoes differential processing, which may account for the differential localization once cleaved. Determining whether these or other mechanisms are involved in this process is the focus of future studies.

Nuclear translocation of cleaved caspase 3 as a harbinger of apoptosis has been noted in rat neuronal cells (50), human cervical epithelial cells (30), human epithelial hepatocytes (27, 28), and human epithelial small cell lung cancer cells (29). Interestingly, the majority of cell types that demonstrate this phenomenon are parenchymal epithelial cells in origin. It is also intriguing that, in hematopoietic cells, which undergo spontaneous apoptosis (i.e., human monocytes), nuclear translocation of cleaved caspase 3 does not occur (49), suggesting that a non–caspase 3–mediated mechanism of programmed cell death is occurring (47). Although our *in vivo* experiments show cleaved caspase 3 translocated to the nucleus (WT conditions) in response to LPS (Figures 3 and 4), the cellular compartment(s) responsible for this is/are not clear. However, as we failed to demonstrate appreciable epithelial barrier disruption, we chose to investigate the endothelial cellular compartment. We clearly demonstrate that, in HMVECs, cleaved caspase 3 translocates to the nucleus in the execution of apoptosis (Figure 5). It is possible that, in our model system, other cell types also demonstrate nuclear translocation of cleaved caspase 3; however, a full characterization of the different cellular compartments is beyond the scope of this study.

In summary, this study demonstrates that, in a sepsis model of lung injury, apoptosis is a key feature associated with nuclear translocation of cleaved caspase 3. We further show that MK2 plays a critical role in the development of apoptosis and lung injury, and its effects on apoptosis are in part related to its ability to regulate nuclear translocation of cleaved caspase 3. The ability to avoid apoptosis by regulating cellular localization of key effector enzymes, rather than preventing activation of the apoptotic cascade, brings the possibility for novel therapeutic targets for ALI as well as other disease states where apoptosis is a key pathogenic factor. ■

Author disclosures are available with the text of this article at www.atsjournals.org.

Acknowledgments: The authors thank the Ross confocal microscope facility and the Bayview confocal microscope facility for technical support, Dr. William Checkley and Dr. Keri Altoff for assistance in data analysis, and Dr. R. M. Tuder for manuscript review.

References

1. Rubenfeld GD, Caldwell E, Peabody E, Weaver J, Martin DP, Neff M, Stern EJ, Hudson LD. Incidence and outcomes of acute lung injury. *N Engl J Med* 2005;353:1685–1693.
2. Hudson LD, Milberg JA, Anardi D, Maunder RJ. Clinical risks for development of the acute respiratory distress syndrome. *Am J Respir Crit Care Med* 1995;151:293–301.
3. Roupie E, Lepage E, Wysocki M, Fagon JY, Chastre J, Dreyfuss D, Mentec H, Carlet J, Brun-Buisson C, Lemaire F, *et al*. Prevalence, etiologies and outcome of the acute respiratory distress syndrome among hypoxemic ventilated patients. SRLF Collaborative Group on Mechanical Ventilation. Societe de Reanimation de Langue Francaise. *Intensive Care Med* 1999;25:920–929.
4. Ware LB, Matthay MA. The acute respiratory distress syndrome. *N Engl J Med* 2000;342:1334–1349.
5. MacIntyre NR. Current issues in mechanical ventilation for respiratory failure. *Chest* 2005;128(5 Suppl 2):561S–567S.
6. Tang PS, Mura M, Seth R, Liu M. Acute lung injury and cell death: how many ways can cells die? *Am J Physiol Lung Cell Mol Physiol* 2008; 294:L632–L641.
7. Le A, Damico R, Damarla M, Boueiz A, Pae HH, Skirball J, Hasan E, Peng X, Chesley A, Crow MT, *et al*. Alveolar cell apoptosis is dependent on p38 MAP kinase–mediated activation of xanthine oxidoreductase in ventilator-induced lung injury. *J Appl Physiol* 2008;105:1282–1290.
8. Li LF, Liao SK, Ko YS, Lee CH, Quinn DA. Hyperoxia increases ventilator-induced lung injury via mitogen-activated protein kinases: a prospective, controlled animal experiment. *Crit Care* 2007;11:R25.
9. Vaschetto R, Kuiper JW, Chiang SR, Haitsma JJ, Juco JW, Uhlig S, Plotz FB, Della Corte F, Zhang H, Slutsky AS. Inhibition of poly(adenosine diphosphate-ribose) polymerase attenuates ventilator-induced lung injury. *Anesthesiology* 2008;108:261–268.
10. Fujita M, Kuwano K, Kunitake R, Hagimoto N, Miyazaki H, Kaneko Y, Kawasaki M, Maeyama T, Hara N. Endothelial cell apoptosis in lipopolysaccharide-induced lung injury in mice. *Int Arch Allergy Immunol* 1998;117:202–208.

11. Imai Y, Parodo J, Kajikawa O, de Perrot M, Fischer S, Edwards V, Cutz E, Liu M, Keshavjee S, Martin TR, *et al*. Injurious mechanical ventilation and end-organ epithelial cell apoptosis and organ dysfunction in an experimental model of acute respiratory distress syndrome. *JAMA* 2003;289:2104–2112.
12. Dolinay T, Wu W, Kaminski N, Ifedigbo E, Kaynar AM, Szilasi M, Watkins SC, Ryter SW, Hoetzel A, Choi AM. Mitogen-activated protein kinases regulate susceptibility to ventilator-induced lung injury. *PLoS One* 2008;3:e1601.
13. Boatright KM, Salvesen GS. Mechanisms of caspase activation. *Curr Opin Cell Biol* 2003;15:725–731.
14. Le Berre R, Faure K, Fauvel H, Viget NB, Ader F, Prangere T, Thomas AM, Leroy X, Pittet JF, Marchetti P, *et al*. Apoptosis inhibition in *P. aeruginosa*–induced lung injury influences lung fluid balance. *Intensive Care Med* 2004;30:1204–1211.
15. Kawasaki M, Kuwano K, Hagimoto N, Matsuba T, Kunitake R, Tanaka T, Maeyama T, Hara N. Protection from lethal apoptosis in lipopolysaccharide-induced acute lung injury in mice by a caspase inhibitor. *Am J Pathol* 2000;157:597–603.
16. Dolinay T, Szilasi M, Liu M, Choi AM. Inhaled carbon monoxide confers antiinflammatory effects against ventilator-induced lung injury. *Am J Respir Crit Care Med* 2004;170:613–620.
17. Damarla M, Hasan E, Boueiz A, Le A, Pae HH, Montouchet C, Kolb T, Simms T, Myers A, Kayyali US, *et al*. Mitogen activated protein kinase activated protein kinase 2 regulates actin polymerization and vascular leak in ventilator associated lung injury. *PLoS One* 2009;4:e4600.
18. Yin T, Sandhu G, Wolfgang CD, Burrier A, Webb RL, Rigel DF, Hai T, Whelan J. Tissue-specific pattern of stress kinase activation in ischemic/reperfused heart and kidney. *J Biol Chem* 1997;272: 19943–19950.
19. So KS, Oh JE, Han JH, Jung HK, Lee YS, Kim SH, Chun YJ, Kim MY. Induction of apoptosis by a stilbene analog involves BAX translocation regulated by p38 MAPK and AKT. *Arch Pharm Res* 2008;31:438–444.
20. Kotlyarov A, Neininger A, Schubert C, Eckert R, Birchmeier C, Volk HD, Gaestel M. MAPKAP kinase 2 is essential for LPS-induced TNF-alpha biosynthesis. *Nat Cell Biol* 1999;1:94–97.
21. Shiroto K, Otani H, Yamamoto F, Huang CK, Maulik N, Das DK. MK2 (−/−) gene knockout mouse hearts carry anti-apoptotic signal and are resistant to ischemia reperfusion injury. *J Mol Cell Cardiol* 2005; 38:93–97.
22. Yardeni T, Eckhaus M, Morris HD, Huizing M, Hoogstraten-Miller S. Retro-orbital injections in mice. *Lab Anim (NY)* 2011;40:155–160.
23. Schmidt EP, Yang Y, Janssen WJ, Gandjeva A, Perez MJ, Barthel L, Zemans RL, Bowman JC, Koyanagi DE, Yunt ZX, *et al*. The pulmonary endothelial glycocalyx regulates neutrophil adhesion and lung injury during experimental sepsis. *Nat Med* 2012;18:1217–1223.
24. Tasaka S, Koh H, Yamada W, Shimizu M, Ogawa Y, Hasegawa N, Yamaguchi K, Ishii Y, Richer SE, Doerschuk CM, *et al*. Attenuation of endotoxin-induced acute lung injury by the Rho-associated kinase inhibitor, Y-27632. *Am J Respir Cell Mol Biol* 2005;32:504–510.
25. Han Z, Hendrickson EA, Bremner TA, Wyche JH. A sequential two-step mechanism for the production of the mature p17:p12 form of caspase-3 *in vitro*. *J Biol Chem* 1997;272:13432–13436.
26. Zhivotovsky B, Samali A, Gahm A, Orrenius S. Caspases: their intracellular localization and translocation during apoptosis. *Cell Death Differ* 1999;6:644–651.
27. Kamada S, Kikkawa U, Tsujimoto Y, Hunter T. A-kinase–anchoring protein 95 functions as a potential carrier for the nuclear translocation of active caspase 3 through an enzyme–substrate–like association. *Mol Cell Biol* 2005;25:9469–9477.
28. Kamada S, Kikkawa U, Tsujimoto Y, Hunter T. Nuclear translocation of caspase-3 is dependent on its proteolytic activation and recognition of a substrate-like protein(s). *J Biol Chem* 2005;280:857–860.
29. Joseph B, Ekedahl J, Lewensohn R, Marchetti P, Formstecher P, Zhivotovsky B. Defective caspase-3 relocalization in non–small cell lung carcinoma. *Oncogene* 2001;20:2877–2888.
30. Luo M, Lu Z, Sun H, Yuan K, Zhang Q, Meng S, Wang F, Guo H, Ju X, Liu Y, *et al*. Nuclear entry of active caspase-3 is facilitated by its p3-recognition–based specific cleavage activity. *Cell Res* 2010;20: 211–222.
31. Matute-Bello G, Frevert CW, Martin TR. Animal models of acute lung injury. *Am J Physiol Lung Cell Mol Physiol* 2008;295:L379–L399.
32. Damico R, Simms T, Kim BS, Tekeste Z, Amankwan H, Damarla M, Hassoun PM. p53 mediates cigarette smoke–induced apoptosis of pulmonary endothelial cells: inhibitory effects of macrophage migration inhibitor factor. *Am J Respir Cell Mol Biol* 2011;44:323–332.
33. Matute-Bello G, Martin TR. Science review: apoptosis in acute lung injury. *Crit Care* 2003;7:355–358.
34. Martin TR, Nakamura M, Matute-Bello G. The role of apoptosis in acute lung injury. *Crit Care Med* 2003;31(4Suppl):S184–S188.
35. Hirahara N, Edamatsu T, Fujieda A, Fujioka M, Wada T, Tajima Y. Protein-bound polysaccharide-K (PSK) induces apoptosis via p38 mitogen-activated protein kinase pathway in promyelomonocytic leukemia HL-60 cells. *Anticancer Res* 2012;32:2631–2637.
36. Ferrari G, Terushkin V, Wolff MJ, Zhang X, Valacca C, Poggio P, Pintucci G, Mignatti P. TGF-β1 induces endothelial cell apoptosis by shifting VEGF activation of p38MAPK from the prosurvival p38β to proapoptotic p38α. *Mol Cancer Res* 2012;10:605–614.
37. Ghatan S, Larner S, Kinoshita Y, Hetman M, Patel L, Xia Z, Youle RJ, Morrison RS. P38 MAP kinase mediates BAX translocation in nitric oxide–induced apoptosis in neurons. *J Cell Biol* 2000;150:335–347.
38. Mehlen P. Schulze Osthoff K, Arrigo AP. Small stress proteins as novel regulators of apoptosis—heat shock protein 27 blocks fas/apo-1– and staurosporine-induced cell death. *J Biol Chem* 1996;271:16510–16514.
39. Chen SW, Park SW, Kim M, Brown KM, D'Agati VD, Lee HT. Human heat shock protein 27 overexpressing mice are protected against hepatic ischemia and reperfusion injury. *Transplantation* 2009;87:1478–1487.
40. Hollander JM, Martin JL, Belke DD, Scott BT, Swanson E, Krishnamoorthy V, Dillmann WH. Overexpression of wild-type heat shock protein 27 and a nonphosphorylatable heat shock protein 27 mutant protects against ischemia/reperfusion injury in a transgenic mouse model. *Circulation* 2004;110:3544–3552.
41. Park SW, Chen SW, Kim M, D'Agati VD, Lee HT. Human heat shock protein 27–overexpressing mice are protected against acute kidney injury after hepatic ischemia and reperfusion. *Am J Physiol Renal Physiol* 2009;297:F885–F894.
42. Paul C, Manero F, Gonin S, Kretz-Remy C, Virot S, Arrigo AP. Hsp27 as a negative regulator of cytochrome C release. *Mol Cell Biol* 2002;22: 816–834.
43. Samali A, Robertson JD, Peterson E, Manero F, van Zeijl L, Paul C, Cotgreave IA, Arrigo AP, Orrenius S. Hsp27 protects mitochondria of thermotolerant cells against apoptotic stimuli. *Cell Stress Chaperones* 2001;6:49–58.
44. Concannon CG, Orrenius S, Samali A. Hsp27 inhibits cytochrome C–mediated caspase activation by sequestering both pro–caspase-3 and cytochrome C. *Gene Expr* 2001;9:195–201.
45. De Vos M, Schreiber V, Dantzer F. The diverse roles and clinical relevance of PARPs in DNA damage repair: current state of the art. *Biochem Pharmacol* 2012;84:137–146.
46. Decker P, Muller S. Modulating poly (ADP-ribose) polymerase activity: potential for the prevention and therapy of pathogenic situations involving DNA damage and oxidative stress. *Curr Pharm Biotechnol* 2002;3:275–283.
47. Galluzzi L, Vitale I, Abrams JM, Alnemri ES, Baehrecke EH, Blagosklonny MV, Dawson TM, Dawson VL, El-Deiry WS, Fulda S, *et al*. Molecular definitions of cell death subroutines: recommendations of the Nomenclature Committee on Cell Death 2012. *Cell Death Differ* 2012;19:107–120.
48. Petrilli V, Herceg Z, Hassa PO, Patel NS, Di Paola R, Cortes U, Dugo L, Filipe HM, Thiemermann C, Hottiger MO, *et al*. Noncleavable poly (ADP-ribose) polymerase-1 regulates the inflammation response in mice. *J Clin Invest* 2004;114:1072–1081.
49. Voss OH, Batra S, Kolattukudy SJ, Gonzalez-Mejia ME, Smith JB, Doseff AI. Binding of caspase-3 prodomain to heat shock protein 27 regulates monocyte apoptosis by inhibiting caspase-3 proteolytic activation. *J Biol Chem* 2007;282:25088–25099.
50. Cao G, Pei W, Lan J, Stetler RA, Luo Y, Nagayama T, Graham SH, Yin XM, Simon RP, Chen J. Caspase-activated DNase/DNA fragmentation factor 40 mediates apoptotic DNA fragmentation in transient cerebral ischemia and in neuronal cultures. *J Neurosci* 2001;21:4678–4690.